

# A Novel Method for Lateral Vehicle Localization by Omni-Cameras for Car Driving Assistance\*

Chih-Jen Wu<sup>1</sup> and Wen-Hsiang Tsai<sup>1,2</sup>

<sup>1</sup> Institute of Computer Science and Engineering, National Chiao Tung University, Taiwan  
gis91813@cis.nctu.edu.tw

<sup>2</sup> Department of Information Communication, Asia University, Taiwan  
whtsai@cis.nctu.edu.tw

**Abstract.** A lateral vehicle localization method by omni-image analysis is proposed for car driving assistance. The method estimates analytically the position and orientation of a lateral vehicle by utilizing the geometric properties of a circular-shaped wheel image of the lateral car taken by a single omni-camera with a hyperboloidal-shaped mirror. Analytical solutions are made possible for fast computation by a special arrangement of affixing the omni-camera on the frontal car bumper at the height of the wheel. Experimental results showing good data estimation precision are included to prove the feasibility of the proposed method.

**Keywords:** vehicle localization, hyperboloidal-shaped mirror, omni-camera, circle, car wheel.

## 1 Introduction

Car driving assistance using traditional cameras has been studied intensively [1-4]. Recently, omni-cameras with wider views become popular. They are more suitable for car driving assistance because fewer cameras need be equipped. For example, Lai and Tsai [3] affixed a traditional camera on the right-frontal side of a *host car* to take the image of a *lateral car*. To acquire a full frontal view, two more traditional cameras should be used. Instead, one frontal omni-camera is sufficient. Additionally, car wheels are circular-shaped, providing geometric hints for lateral car localization [3]. However, when a circle appears in an omni-image, it becomes irregular in shape and cannot be described mathematically [5], leading to difficulty of extending the existing vehicle localization methods for omni-images.

In this study, we try to solve this problem. The omni-camera is equipped on the frontal bumper *at the height of the wheel* so that the mathematics involved in circular-shape image analysis becomes maneuverable to get analytic solutions for fast computation. In the following, the proposed method is described in Section 2, followed by some experimental results in Section 3 and conclusions in Section 4.

---

\* This work was supported financially by the Ministry of Economic Affairs under Project No. MOEA 97-EC-17-A-02-S1-032 in Technology Development Program for Academia.

## 2 Lateral Car Localization by Frontal Omni-Camera

The basic idea of the proposed method is to utilize the geometric properties of a circular-shaped wheel image of the lateral car taken by a single omni-camera to estimate the position and orientation of the lateral car with respect to the host car. The omni-camera, affixed to the frontal bumper of the host car at the height of the wheel, includes a hyperboloidal-shaped mirror. Also, the optical axis of the camera is set to be horizontal to the ground plane. Such an arrangement of the camera makes the resulting irregular shape of the wheel in the omni-image to be extractable as an ellipse using the Hough transform, as proved in [5]. More details are described by the following algorithm.

### Algorithm 1. Lateral car localization by a frontal omni-camera on a host car.

- Step 1. Affix an omni-camera to the frontal bumper of the host car at the height of the wheel center with the camera's optical axis adjusted to be horizontal to the ground plane and pointing to the frontal direction of the host car.
- Step 2. Take an image of a wheel of the lateral car and find out the vertical height  $h$  of the wheel in the image.
- Step 3. With the radius of the wheel and the value of  $h$  as input, estimate the position of the lateral car (details described in Section 2.1).
- Step 4. Find out the farthest and the closest points,  $I_f$  and  $I_c$ , of the wheel in the image with respect to the image center.
- Step 5. With  $I_f$  and  $I_c$  as input, derive the direction of the lateral car with respect to the host car (details described in Section 2.2).

### 2.1 Estimation of Lateral Car Position Using Rotational Invariance Property

The coordinate systems involved in an omni-camera system, including a traditional perspective camera and a hyperboloidal-shaped mirror, are depicted in Fig. 1(a), where the omni-camera and the image coordinates are specified by  $(X, Y, Z)$ , and  $(u, v)$ , respectively. The perspective camera and the mirror are properly aligned, as assumed, so that the omni-camera becomes a *single-viewpoint* system, and that the optical axis of the perspective camera coincides with the mirror axis which is the line going through the mirror center and perpendicular to the mirror base.

The middle point between the camera lens center  $O_l$  and the mirror focus point  $O_m$  is taken to be the origin  $O_a$  of the omni-camera coordinate system. The hyperboloidal mirror shape may so be described by

$$\frac{r^2}{a^2} - \frac{Z^2}{b^2} = -1, \quad r = \sqrt{X^2 + Y^2} \quad (1)$$

and  $O_m$  is located at  $(0, 0, -c)$  and  $O_l$  at  $(0, 0, +c)$  in the camera coordinate system where  $c = \sqrt{a^2 + b^2}$ . The relationship between  $(u, v)$  and  $(X, Y, Z)$  may be described [5] by

$$u = \frac{Xf(b^2 - c^2)}{(b^2 + c^2)(Z - c) - 2bc\sqrt{(Z - c)^2 + X^2 + Y^2}};$$

$$v = \frac{Yf(b^2 - c^2)}{(b^2 + c^2)(Z - c) - 2bc\sqrt{(Z - c)^2 + X^2 + Y^2}} \quad (2)$$

where  $f$  is the camera's focal length, and  $b$ ,  $c$ , and  $f$  are parameters assumed to be known in advance.

Also, as illustrated in Fig. 1(b), the omni-camera is affixed to the car bumper with the  $Z$ -axis of the omni-camera adjusted to be at the height of the wheel center, the negative  $Z$ -axis directed to the car driving direction, and the  $Y$ -axis set perpendicular to the ground surface. A wheel coordinate system  $x$ - $y$ - $z$  is defined on the left-frontal wheel of the lateral car with its origin  $O_w$  being the wheel center and its  $x$ - $y$  plane being the wheel plane. The orientation of the wheel plane is denoted by  $\theta$  with  $\theta = 0^\circ$  meaning that the lateral car moves in parallel. The wheel's radius is assumed to be  $R$ . Then, defining  $(X_c, Y_c, Z_c)$  as the wheel center's coordinates in the omni-camera coordinate system, we get

$$Y_c = 0; \quad (3)$$

$$Y = y. \quad (4)$$

From the above omni-camera geometry, it is not difficult to figure out the validity of the so-called *rotational invariance* property, which means that the angle of an incoming light ray formed by a space point at coordinates  $(X, Y, Z)$  onto the mirror surface in the omni-camera coordinate system is identical to the angle of the corresponding image point at coordinates  $(u, v)$  in the image coordinate system, leading to the following equality:

$$\frac{v}{u} = \frac{Y}{X}. \quad (5)$$

The lateral car localization problem now is to derive the wheel position and orientation parameters  $X_c$ ,  $Z_c$ , and  $\theta$  of the lateral car in the omni-camera coordinate system. First, define  $P_1$  through  $P_4$  as the four extreme points on the wheel circle so that the segments  $\overline{P_1P_2}$  and  $\overline{P_3P_4}$  are perpendicular and parallel to the ground surface, respectively, as illustrated by Fig. 2. Obviously,  $P_1$  and  $P_2$  are at  $(X_c, +R, Z_c)$  and  $(X_c, -R, Z_c)$ , respectively. Next, it can be figured out that the  $Y$ -coordinates of  $P_3$  and  $P_4$  are equal to  $Y_c$ , which is zero, because the wheel center  $O_w$  at  $(X_c, Y_c, Z_c)$  is at the height of the omni-camera coordinate system origin  $O_a$  at coordinates  $(0, 0, 0)$ , as assumed. Denote the image point corresponding to  $P_i$  as  $I_i$  and its coordinates as  $(u_i, v_i)$ ,  $i = 1, 2, 3, 4$ . Applying (5) to  $I_1$  and  $I_2$ , we get

$$\frac{v_1}{u_1} = \frac{R}{X_c}; \quad \frac{v_2}{u_2} = \frac{-R}{X_c}. \quad (6)$$

Also, from (2) and the omni-camera coordinates of  $P_1$  and  $P_2$ , we get

$$u_1 = u_2. \quad (7)$$

Combining (6) and (7), we get the solution for  $X_c$  as

$$X_c = \frac{2R}{v_1 - v_2} u_1. \quad (8)$$

Note that  $v_1 - v_2$  is just the value  $h$  mentioned in Step 3 of Algorithm 1.

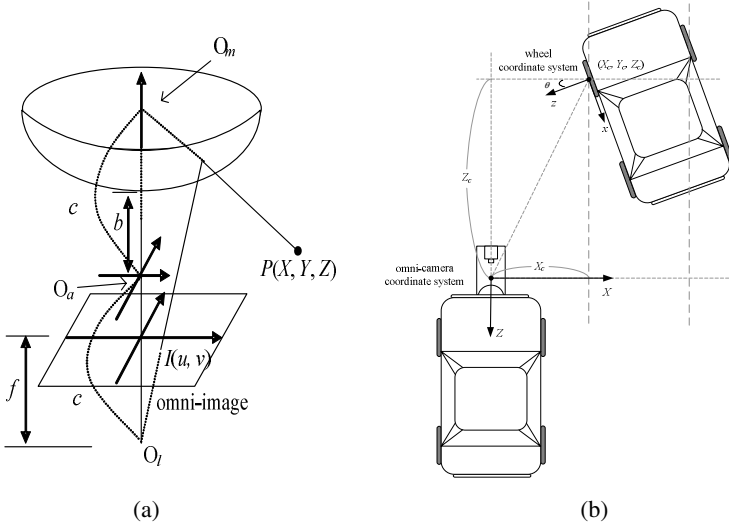


**Fig. 1.** Relative coordinate systems. (a) Omni-camera and image coordinate systems. (b) Omni-camera and wheel coordinate systems.

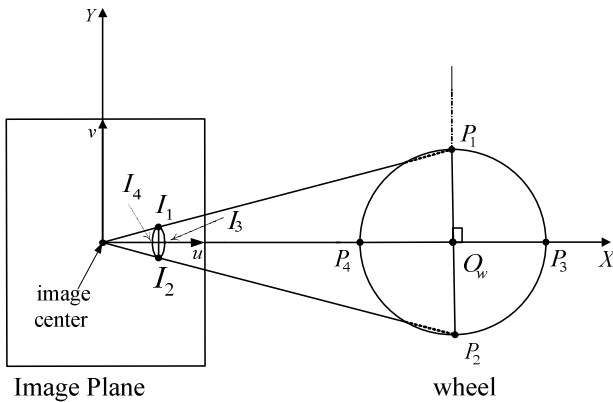


**Fig. 2.** Definition of corresponding image and space points

To derive  $Z_c$ , let

$$Z_c' = Z_c - c. \tag{9}$$

Then, (2) for  $I_1$  may be transformed into

$$[u_1^2(b^2 + c^2)^2 - u_1^2(-2bc)^2](Z_c')^2 - [2u_1X_c f(b^2 - c^2)(b^2 + c^2)](Z_c') + [f^2(b^2 - c^2)^2 X_c^2 - u_1^2(-2bc)^2 X_c^2] = 0$$

which leads to

$$A(Z_c')^2 + B(Z_c') + C = 0 \tag{10}$$

where

$$\begin{aligned} A &= u_1^2(b^2 - c^2)^2; \\ B &= -2u_1X_c f(b^2 - c^2)(b^2 + c^2); \\ C &= X_c^2[f^2(b^2 - c^2)^2 - 4b^2c^2u_1^2]. \end{aligned} \quad (11)$$

So, we get

$$Z_c' = \frac{-B \pm \sqrt{B^2 - 4AC}}{2A} \quad (12)$$

which may be simplified to be

$$Z_c' = \frac{X_c[f(b^2 + c^2) \pm 2bc\sqrt{f^2 + u_1^2}]}{u_1(b^2 - c^2)}. \quad (13)$$

With the solution for  $X_c$  in (8),  $Z_c' = Z_c - c$  in (9), and the equation of (13) above, we get finally the solution for  $Z_c$  as

$$\begin{aligned} Z_c &= Z_c' + c \\ &= \frac{X_c[f(b^2 + c^2) \pm 2bc\sqrt{f^2 + u_1^2}]}{u_1(b^2 - c^2)} + c \\ &= \frac{2R[f(b^2 + c^2) \pm 2bc\sqrt{f^2 + u_1^2}]}{(v_1 - v_2)(b^2 - c^2)} + c. \end{aligned} \quad (14)$$

The sign (+ or -) in (14) may be decided experimentally.

## 2.2 Estimation of Lateral Car Orientation Using Wheel Shape Information

Now, we want to use the image coordinates  $(u_3, v_3)$  and  $(u_4, v_4)$  of  $I_3$  and  $I_4$  (denoted as  $I_f$  and  $I_c$  respectively in Step 4 of Algorithm 1) to derive the wheel orientation  $\theta$  based on the values of  $X_c$  and  $Z_c$  obtained previously. First, according to (2) and because  $Y_3 = Y_4 = Y_c = 0$ , we get  $v_3 = v_4 = 0$  and

$$u_3 = \frac{X_3 f(b^2 - c^2)}{(b^2 + c^2)(Z_3 - c) - 2bc\sqrt{(Z_3 - c)^2 + X_3^2 + Y_3^2}}; \quad (15)$$

$$u_4 = \frac{X_4 f(b^2 - c^2)}{(b^2 + c^2)(Z_4 - c) - 2bc\sqrt{(Z_4 - c)^2 + X_4^2 + Y_4^2}}. \quad (16)$$

Also, define

$$Z_3' = Z_3 - c; \quad (17)$$

$$Z_4' = Z_4 - c. \quad (18)$$

Using (15) and (16) and through a similar process to that for deriving (13), we get

$$Z_3' = \frac{X_3[f(b^2 + c^2) \pm 2bc\sqrt{f^2 + u_3^2}]}{u_3(b^2 - c^2)}; \tag{19}$$

$$Z_4' = \frac{X_4[f(b^2 + c^2) \pm 2bc\sqrt{f^2 + u_4^2}]}{u_4(b^2 - c^2)}. \tag{20}$$

Furthermore, with the middle point of  $\overline{P_3P_4}$  as the wheel center  $O_w$ , we get

$$X_4 = 2X_c - X_3; \tag{21}$$

$$Z_4 = 2Z_c - Z_3. \tag{22}$$

Combining (17), (18) and (22), we have

$$Z_4' = 2Z_c - Z_3' - 2c. \tag{23}$$

Also, (19) and (20) may be transformed into

$$Z_3' = X_3A_3; \tag{24}$$

$$Z_4' = X_4A_4 \tag{25}$$

where

$$A_3 = \frac{[f(b^2 + c^2) \pm 2bc\sqrt{f^2 + u_3^2}]}{u_3(b^2 - c^2)}; \tag{26}$$

$$A_4 = \frac{[f(b^2 + c^2) \pm 2bc\sqrt{f^2 + u_4^2}]}{u_4(b^2 - c^2)}. \tag{27}$$

Combining (21) and (23) through (25), we get

$$X_3 = 2(Z_c - X_cA_4 - c)/(A_3 - A_4). \tag{28}$$

And from (17), (24), and (28), we get

$$Z_3 = (2Z_cA_3 - 2X_cA_3A_4 - cA_3 - cA_4)/(A_3 - A_4). \tag{29}$$

And from (22) and (29), we get

$$Z_4 = (2X_cA_3A_4 + cA_3 + cA_4 - 2Z_cA_4)/(A_3 - A_4). \tag{30}$$

Accordingly, from (25) we get

$$\begin{aligned} X_4 &= Z_4'/A_4 = (Z_4 - c)/A_4 \\ &= (2X_cA_3A_4 + cA_3 + cA_4 - 2Z_cA_4 - c)/(A_3 - A_4)A_4. \end{aligned} \tag{31}$$

With (28) through (31), we finally get the desired result

$$\theta = \tan^{-1}\left(\frac{X_3 - X_4}{Z_3 - Z_4}\right).$$

### 3 Experimental Results

In our experiments a set of real location data of a lateral car in different postures were measured before corresponding images were taken to estimate the posture parameters  $X_c$ ,  $Z_c$ , and  $\theta$  using the previously-derived equations. An example of the acquired images is shown in Fig. 3, in which detection of a wheel shape as an ellipse is also shown. Some estimation results are shown in Table 1. The error for  $X_c$  or  $Z_c$  is computed as the ratio of the difference between the estimated value and the real one with respect to the real value. And the angle error for  $\theta$  is computed similarly but with respect to  $180^\circ$  which is the angle range of the lateral car. The table shows that the estimated values of  $X_c$  and  $Y_c$  are within 5% errors which are good enough for practical applications. But some angle errors are larger. The reason is that the wheel size in the images of these cases appeared to be small, so that the estimated angle  $\theta$  is sensitive to the width of the horizontal wheel diameter  $P_3P_4$ .

Moreover, in Section 2.1 the radius of the wheel should be known in advance for estimating the vehicle location. However, in real cases of applying the proposed vehicle localization method, the type of the wheel on the vehicle is unknown in advance. A solution is to assume an average wheel radius, which is 20.75cm according to our measurement of a lot of car wheel radiuses. But this way will introduce errors in the estimated position values. Therefore, a simulation experiment was conducted to test

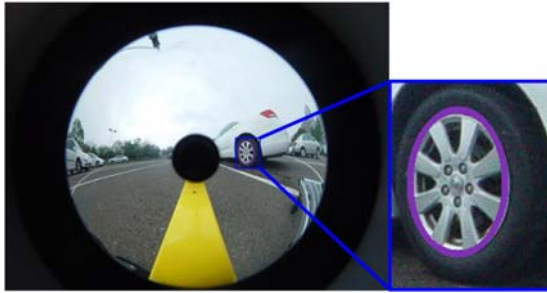


**Fig. 3.** A lateral car image with wheel shape detected as an elliptical shape

**Table 1.** Lateral car location estimation results

<i>real <math>X_c</math></i> (cm)	<i>estimated <math>X_c</math></i> (cm)	<i>error ratio</i> <i>of <math>X_c</math></i>	<i>real <math>Z_c</math></i> (cm)	<i>estimated <math>Z_c</math></i> (cm)	<i>error</i> <i>ratio of <math>Z_c</math></i>	<i>real <math>\theta</math></i> (degree)	<i>estimated <math>\theta</math></i> (degree)	<i>angle error</i> (degree)
-104.3	-99.7	4.4%	-40.9	-39.3	4.0%	-5	-6	0.6%
-390.4	-382.4	2.2%	-87.2	-87.7	0.6%	15	13	1.1%
-464.9	-478.0	4.8%	-494.9	-502.7	1.6%	22	38	8.9%
-137.7	-138.4	0.7%	-159.9	-166.6	4.2%	9	21	6.7%
-407.0	-419.0	4.3%	-115.2	-112.5	2.3%	33	22	6.1%
608.0	606.8	0.6%	-235.5	-240.3	2.0%	-82	-73	5.0%
<i>average</i> <i>error</i>		2.8%			2.5%			4.7%

**Table 2.** Simulation results of estimating lateral car position using a fixed wheel radius value 20.75 cm

input radius of wheel (cm)	19.75		20.41		21.08		21.75	
position coordinates	X	Z	X	Z	X	Z	X	Z
input real values (cm)	400	100	400	100	400	100	400	100
estimated values (cm)	419.24	104.81	405.55	101.39	392.73	98.18	380.69	95.17
error ratio	4.81%	4.81%	1.39%	1.39%	-1.82%	-1.82%	-4.82%	-4.82%

whether the errors are tolerable or not. For this, first we project the wheel shape of a lateral car onto the image plane using a set of different real wheel radius parameters (ranging from 19.75cm to 21.75cm as measured by us). Then the proposed method was applied to estimate the position of the lateral car, under the assumption that the radius of the wheel of the car is of the above-mentioned average value 20.75cm. The results are shown in Table 2. The average error rates of the position parameters are all smaller than 5%, so the use of a fixed wheel radius in deriving the lateral car location is considered feasible in practice.

## 4 Conclusions

A lateral vehicle localization method by the use of a single frontal omni-camera has been proposed. The basic concept is to affix a single omni-camera on the bumper at the height of the wheel so that the mathematics involved in the analysis of the irregular shape of the circular wheel in the image becomes maneuverable, leading to the possibility of deriving analytic solutions. Experimental results show that most location estimation results are with error ratios smaller than 6%, which means that the proposed method is feasible for practical applications.

## References

1. Lin, H.H., Lin, J.H.: A Visual Positioning System for Vehicle or Mobile Robot Navigation. *IEICE Transactions on Information and Systems* E89-D(7), 2109–2116 (2006)
2. Sakurai, K., Kyo, S., Okazaki, S.: Overtaking Vehicle Detection Method and Its Implementation Using IMAPCAR Highly Parallel Image Processor. *IEICE Transactions on Information and Systems* E91-D(7), 1899–1905 (2008)
3. Lai, C.C., Tsai, W.H.: Estimation of Moving Vehicle Locations Using Wheel Shape Information in Single 2-D Lateral Vehicle Images by 3-D Computer Vision Techniques. *Robotics and Computer Integrated Manufacturing* 15, 111–120 (1999)
4. Cao, Y., Renfrew, A., Cook, P.: Vehicle Motion Analysis Based on a Monocular Vision System. In: *Proceedings of 2008 Road Transport Information and Control and ITS Conference*, Manchester, UK, pp. 1-6 (2008)
5. Wu, C.J., Tsai, W.H.: Location Estimation for Indoor Autonomous Vehicle Navigation by Omni-Directional Vision Using Circular Landmarks on Ceilings. *Robotics and Autonomous Systems* 57(5), 546–555 (2009)